Korean J. Chem. Eng., **29**(5), 595-600 (2012)
DOI: 10.1007/s11814-011-0216-0

Conditional monitoring of moisture content in a fluidized bed dryer by the acoustic emission signature

Farhad Karimi, Rahmat Sotudeh-Gharebagh†, Reza Zarghami, Mojgan Abbasi, and Navid Mostoufi

Multiphase Systems Research Lab, School of Chemical Engineering, College of Engineering,
University of Tehran, P. O. Box 11155/4563, Tehran, Iran
(*Received 29 April 2011 • accepted 17 August 2011*)

Abstract−Wetted rice particles were dried in a fluidized bed and the corresponding passive acoustic emissions signals (AES) were recorded at a given frequency to study the drying phenomena and bed hydrodynamic changes as well. The results show that the end time of the constant rate zone and the end of the falling rate can be determined from the variation of standard deviation and kurtosis of AES, respectively. Frequency domain analysis was also used to quantify the moisture content of solids. For this end, the original signal was decomposed into ten sub-signals, and it was found that the energy of the 4th sub-signal can be correlated with the moisture content. The results show that the acoustic emission measurement is applicable as a practical method for on-line condition monitoring of drying process in fluidized bed dryers.

Key words: Fluidized Bed Dryer, Moisture Content, Online Monitoring, Acoustic Emission

INTRODUCTION

According to the interesting advantages of fluidized beds, many researchers have investigated these dryer applications in new industrial plants and design aspects of these beds [1-3]. Several methods have been reported in the literature for monitoring fluidized bed hydrodynamics, including pressure fluctuations [4,5], acoustic emissions (AE) [6-9], vibration signature [10-12], three-dimensional X-ray imaging [13] and electrostatic measurements [14,15]. Among the devices used, the acoustic sensors are inexpensive and can withstand a wide range of process conditions. They provide reliable, on-line and non-intrusive monitoring. Nevertheless, difficulties in extracting the information from the acoustic signals hinder the widespread application of AE monitoring [16].

Friesen et al. [17] proposed a method for determining the moisture content (MC) of wheat grains by dropping them from a certain height on a plate and measuring the sound pressure level of the contact. They showed that a correlation exists between the sound level (dB) and the MC and demonstrated that the sound level decreases across the entire frequency range as the MC increases. Vervloet et al. [18] compared passive acoustics and vibration signals with pressure measurements for monitoring gradual process changes in fluidized bed reactors. They measured all signals at frequencies up to 400 Hz. After comparing with pressure fluctuations, they have concluded that both acoustic and vibration measurements may be useful for monitoring purposes, provided that both the sensor and the data analysis method are chosen suitably.

In the gas-solid fluidized beds, the sounds generated by the friction, collisions, fluid turbulence [16], and eruption of bubbles at the bed surface can provide the listener with valuable information on the bed hydrodynamics. Each sound source has one or more specific distinct frequencies in power spectra diagram. Therefore, dominant frequencies of each source, if determined accurately, may show the corresponding phenomena inside of the bed. In addition, a logical relationship may exist between the physical phenomena and the statistical parameters derived from the AE. Therefore, the aim of this study is to test the applicability of passive acoustic emissions for on-line condition monitoring of drying process as a potentially non-intrusive technique. For this purpose, the suitability of statistical and frequency analyses for exploring the acoustic emission signals was also investigated.

EXPERIMENTS

Experiments were performed in a Plexiglas column with an inner diameter of 15 cm and a height of 2 m. The column was equipped with a perforated distributor plate of 435 holes of 7 mm triangle pitch. The whole system was electrically grounded to minimize electrostatic effects. Air at room temperature and atmospheric pressure entered into the column through the distributor, and its flow rate was measured by an orifice plate connected to a water manometer. Bruel & Kjær free-field microphone type 4190 with sensitivity of 50 mV/Pa was used to record the sound signals. The microphone was located 50 cm above the distributor.

Salehi-Nik et al. [9] and Briongos et al. [8] concluded that the measured sound signals are independent from the microphone situation. The microphone produced analogue signals that were conditioned and converted to digital using the B&K PULSE system along with 3560C hardware. The sound measurements were collected using a specific sampling rate of 4,096 Hz during 72 minutes in eighteen periods of 256 s. The sampling frequency was high in order so as not to lose information in the acoustic pressure changes. Nevertheless, cutting off the frequencies above 500 Hz did not change the signals. A high-pass filter was integrated on the signals at 7 Hz.

Wetted rice particles (Geldart B) were added to the bed with the

†To whom correspondence should be addressed.
E-mail: sotudeh@ut.ac.ir

Table 1. Physical property of rice particles

Particle density	Mass	Major diameter	Intermediate diameter	Minor diameter	Mean diameter
(g cm^{-3})		(mm)			
1.136	0.026	8.27	2.85	1.98	3.596
Moisture content as 38% (on dry basis)					
1.152	0.036	8.53	2.68	1.93	3.525

initial aspect ratio equal to 1. Rice was selected as a representative grain due to its economical importance. However, this method can be used for measuring moisture content of other grains as well. Some of the physical properties of rice particles are presented in Table 1. Initially, the superficial gas velocity was raised to 0.8 m/s for approximately 5 min to make sure that no wetted material would stick to the bottom or the wall of the bed and then the bed was operated under the bubbling fluidization regime with 1.1 m/s as the superficial gas velocity. Between any two consecutive periods, air flow was cut to allow measuring reduction of static bed height and determining MC of particles. Wetted particles were then taken out from the bed by scooping the bed material. These samples were weighed and dried for three days at 50 °C in an oven. The MC of the samples was calculated by the weight difference of the samples before and after drying based on the weight of dried particles (dry basis).

METHOD OF ANALYSIS

Different methods have been utilized for processing the signals generated from the fluidized beds. These methods can be divided into three categories: (i) time domain analyses, (ii) frequency domain analyses, and (iii) state-space analyses [18,19]. In the present work, statistical analysis in time domain as well as the frequency domain analysis was used.

1. Time Domain

In the time domain, statistical techniques consider changes of amplitude and frequency of raw data. This technique includes standard deviation, skewness, kurtosis and average cycle frequency (ACF).

The standard deviation (σ) is a measure of the degree to which the data spreads around a mean value defined as follows:

$$\sigma=\sqrt{\frac{1}{n-1}\sum_{i=1}^{n}(x_i-\bar{x})^2} \tag{1}$$

where the mean value is evaluated from:

$$\bar{x}=\frac{1}{n}\sum_{i=1}^{n}x_i \tag{2}$$

Van der Schaaf et al. [20] used standard deviation of pressure fluctuations as a qualitative indicator of the relative bubble size in the bed.

Skewness is a measure of the asymmetry of the probability distribution of a real-valued random variable. A distribution has a positive skew (right-skewed) if the right tail is longer and negative skew (left-skewed) if the left tail is longer. Skewness is calculated from:

$$S=\frac{\sum_{i=1}^{n}(x_i-\bar{x})^3}{(n-1)\sigma^3} \tag{3}$$

Kurtosis, or the fourth moment, is a measure of the relative peakedness of the distribution. Kurtosis is calculated by:

$$K=\frac{\sum_{i=1}^{n}(x_i-\bar{x})^4}{(n-1)\sigma^4} \tag{4}$$

The average cycle frequency (ACF) is defined as the number of cycles in signal fluctuations per second. The number of cycles is equal to half of the time that the signal amplitude crosses its average and is calculated by sign change of the raw date per second. Wormsbecker et al. [21] and Zarghami et al. [19] used ACF of pressure fluctuations to characterize the passing of bubbles in a fluidized bed.

2. Frequency Domain

It is often impossible to observe hydrodynamic changes directly in the signal from the raw data alone [18]. The power spectral density function (PSDF) is a tool to analyze and to characterize the hydrodynamics of fluidized beds and is calculated by:

$$P_{xx}^{i}(f)=\frac{1}{\sum_{n=1}^{N}w^2(n)}\left[\sum_{n=1}^{N}x_i(n)w(n)e^{-j2\pi nf}\right]^2 \tag{5}$$

Johnsson et al. [22] used the shape of the PSDF of pressure fluctuations to determine different modes of bubbling (single, multiple and bursting of bubbles). The averaged power spectrum is:

$$P_{xx}(f)=\frac{1}{L}\sum_{i=1}^{L}P_{xx}^{i}(f) \tag{6}$$

The PSDF has low resolution due to constant width of the analysis window for the whole frequency band of the experiment. Thus, for obtaining a better resolution and more precise frequency information at both low and high frequencies, wavelet transform (WT) analysis can be used. The WT is suitable for analysis of irregular or unsteady data patterns, such as impulses occurring at various time instances. The wavelet transform of a signal f(x) is defined as:

$$W_s f(x)=\int_{-\infty}^{+\infty}f(u)\,\varphi_s(x-u)\,du \tag{7}$$

Where

$$\varphi_s=\frac{1}{s}\varphi\left(\frac{x}{s}\right) \tag{8}$$

For practical implementation, the discrete wavelet transform can be used. The following discrete wave filter functions are constructed corresponding to:

$$DWT(j,k)=\frac{1}{\sqrt{|2^j|}}\int_{-\infty}^{+\infty}x(t)\,\varphi\left(\frac{t-k\cdot 2^j}{2^j}\right)dt \tag{9}$$

The original signal can be decomposed into approximation sub-signals $a_j(t)$ and detailed sub-signals $D_j(t)$ by the theory of Mallat [23]. In this theory, the signal is passed through a series of low-pass and high-pass pairs of filters called quadrature mirror filters. At each step of the decomposition process, the frequency resolution is doubled through filtering and the time resolution is halved through down-sampling. The original signal x(t) can be recovered in terms of the sub-signals of different scales:

$$x(t) \approx a_j(t) + D_j(t) + D_{j-1}(t) + \ldots + D_1(t) \quad (10)$$

The energies of $a_j(t)$ and $D_j(t)$ are evaluated as:

$$E_j^a = \sum_{i=1}^{N} |a_j(t)|^2 \quad (11)$$

$$E_j^D = \sum_{i=1}^{N} |D_j(t)|^2 \quad (12)$$

Therefore, energy distribution of x(t) can be calculated by Eqs. (11) and (12) at various sub-signals. Based on the orthogonality and the energy conservation of the WT, the total energy of the original signal x(t) can be calculated by:

$$E = \sum_{i=1}^{N} |x(t)|^2 = E_j^a + \sum_{j=1}^{j} E_j^D \quad (13)$$

In the present study, the third-order Daubechie's wavelet (Daublet 3) was used as the wavelet function.

RESULTS AND DISCUSSION

Once every 256 s during the 72-minute test, the MC of the solids was measured. These values are shown in Fig. 1. According to the trend of drying process shown in this figure, two periods can be identified:

1. Constant drying rate period: drying is continued until the end of surface moisture at 20 min.

2. Falling-rate period: drying is continued after the end of free moisture on the surface. This transition point, denoted as the critical MC, occurs when a continuous film of moisture cannot be maintained on the surface of the particles. This period continues up to equilibrium moisture content (EMC) is reached. The EMC is the final MC of the grain that can be determined by the temperature and relative humidity (RH) of the air surrounding the grain. This period in industrial dryer usually prevails in the overall drying to EMC. Fig. 1 demonstrates that critical and equilibrium moisture contents are about 23.8% and 10.19% on dry basis (is defined as: $(M_{wet}-M_{dry})/M_{dry}$), respectively.

The drying rate and moisture content of rice particles during the drying rate is shown in Fig. 2. Three regions are shown in this figure. In the first region, the rate of drying is around 0.71%/min and constant. This constant rate continues until 20 minutes of drying as mentioned above. In the second region, referred to as the falling rate region, the drying rate levels off and it almost changes linearly with time until it reaches zero. This occurs at around 60 minutes of drying process, where the equilibrium moisture content is attained (third region).

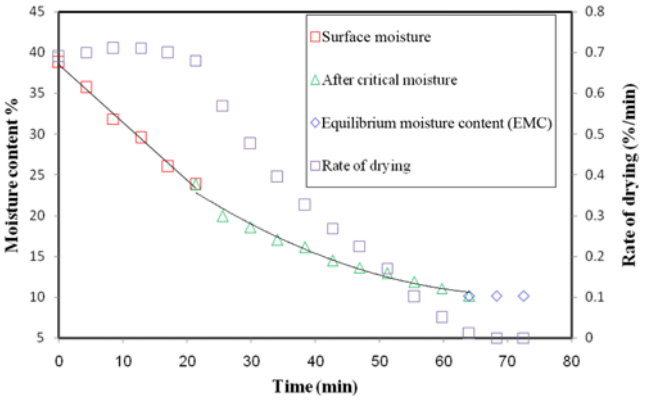

Fig. 2. Evolution of moisture content and drying rate over time.

Based on the visual observations, bubbles were not formed in the bed until the surface moisture vanished. In fact, the liquid bridges prevent particles from freely moving and the air passed through the bed by creating channels. Only after elimination of the surface moisture were the first bubbles visible in the center of the bed, and the bubbles were then evenly distributed in the bed. The same observations were reported by Chaplin et al. [24]. A decrease in static bed height, approximately 5 cm or 33% initial bed height, was also observed during drying process. Variation of the static bed height of the bed during drying is shown in Fig. 1.

During the drying operation, size and number of bubbles are affected by two events:

1. Decreasing the aspect ratio in the bed due to shrinkage of particles. The bubble size decreases in a shallower bed because bubble coalescence is less frequent in order to create large bubbles.

2. Decreasing moisture content causes the particles to become lighter and need lower minimum fluidization velocity; hence, the amount of air going to bubbles becomes greater.

Thus, during the drying process, increasing the excess air leads to an increase in the number of bubbles passing through the bed

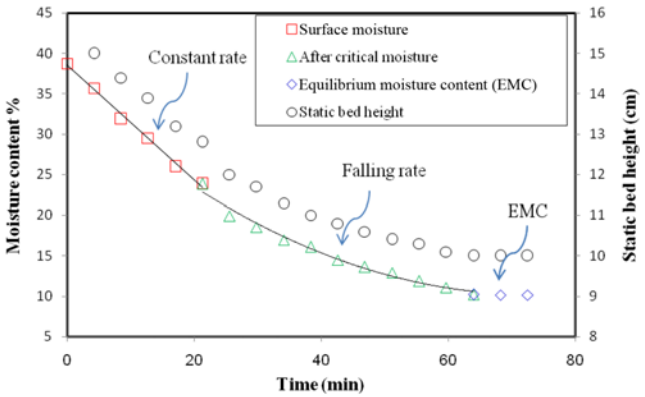

Fig. 1. Moisture content and static bed height over time.

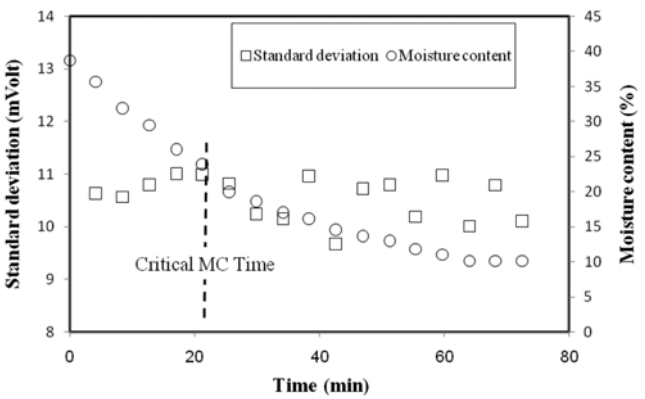

Fig. 3. Standard deviation values and moisture content over time.

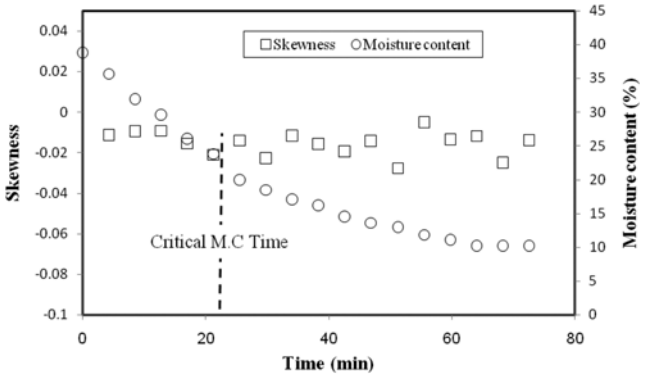

Fig. 4. Skewness values and moisture content over time.

but not the bubble size. Of course, if the decreasing static bed height during operation is not significant, the bubble size can be increased as reported by Wormsbecker et al. [21].

1. Time-domain Analysis

Acoustic emissions were analyzed in the time domain by standard deviation, skewness and kurtosis. Fig. 3 shows standard deviations of acoustic emission signals at every 256 s interval during the drying process. It can be seen in this figure that the standard deviation reaches a maximum at the end of constant rate zone. However, at moisture content below this point, it does not follow a particular trend. Fig. 4 shows the changes of skewness in the course of drying. This figure reveals that there is no specific trend of skewness during the drying process and the skewness is almost constant. Therefore, this parameter cannot be considered for following the changes of MC of particles in fluidized bed dryers.

Another statistical parameter that was used to examine the acoustic emission signals is the fourth central moment, kurtosis. Variation of this parameter during the drying process is demonstrated in Fig. 5. As can be seen, kurtosis of acoustic emission signals shows a small peak near the critical MC. Also, there is a sharp peak near the EMC. Hence, changes of kurtosis can be considered as a criterion in determining the EMC and the end time of drying. Salehi-Nik et al. [9] also reported a sudden rise in the kurtosis at minimum fluidization velocity. Thus, the fourth central moment, or kurtosis, can observe the sudden changes in passive acoustic emissions

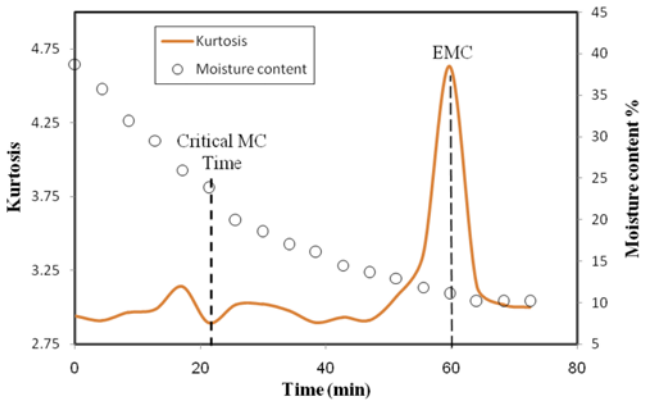

Fig. 5. Kurtosis trend of signals and moisture content curve over time.

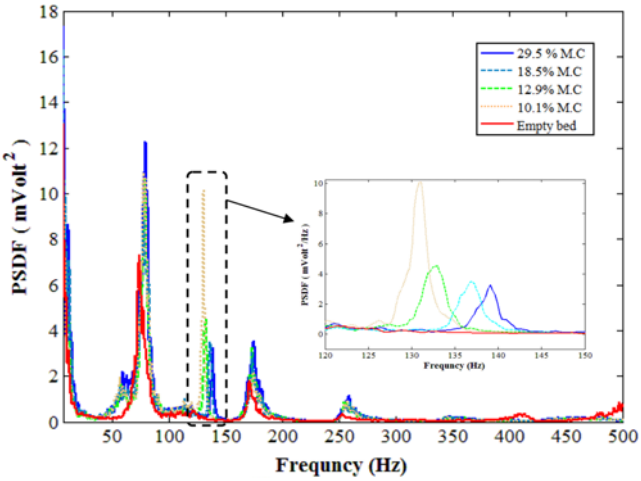

Fig. 6. Fourier transform of acoustic signal of rice particles (Geldart B) in several moisture content (M.C) and the close-ups of the frequency range of 115-165 Hz of the same graphs with the initial aspect ratio of 1.at 1.1 m/s superficial gas velocity.

of fluidized bed properly.

2. Frequency Domain Analysis

The PSDF analysis of sound signals were used to investigate the evolution of sound signals as a function of MC for rice particles in the bubbling regime of fluidization. Fig. 6 shows an overview of the PSDF of sound signals for several MCs during the drying period with the initial aspect ratio of 1 at 1.1 m/s superficial gas velocity. Despite the high-frequency measurements, this figure is drawn up to 500 Hz because no distinct frequencies were seen greater than 500 Hz. Therefore, the sampling frequency for acoustic signals can be selected at 1,000 Hz without losing any information. The sampling frequency should be greater than the twice maximum frequency component within the frequency spectrum [25]. As illustrated in Fig. 6, five frequency peaks can be observed for every PSDF diagram. Each peak can be related to the interaction of several sound source frequencies. Contrary to pressure and vibration signals which have only one distinct frequency in most part of the bubbling regime [11,19], the PSDF diagram of acoustic signals has several distinct frequencies. As mentioned earlier, emission of sound in gas-solid fluidized beds is generated by numerous events such as coalescence of bubbles, bursting of bubbles on the bed surface, friction and collision of particles with the wall and each other and passing of air through the column. Among all these cases, only sound of air passing through the column has a constant value because air velocity was constant in the entire course of drying. Because every sound has specific frequencies in the PSDF diagram and since the PSDF of the empty bed does not show any peak in the frequency range of 115-165 Hz (third distinct frequency rang), it can be concluded that the frequency observed in this range is generated by other sound source factors related to the change in the moisture content of the solids. Although few differences at other peak can be seen, a close-up view of them indicated that their frequency differences are less than the third peak and the third peak is more sensitive to the moisture changes. Due to a direct relationship between sounds and bed hydrodynamic condition, this peak can be chosen as the hydrodynamic peak of

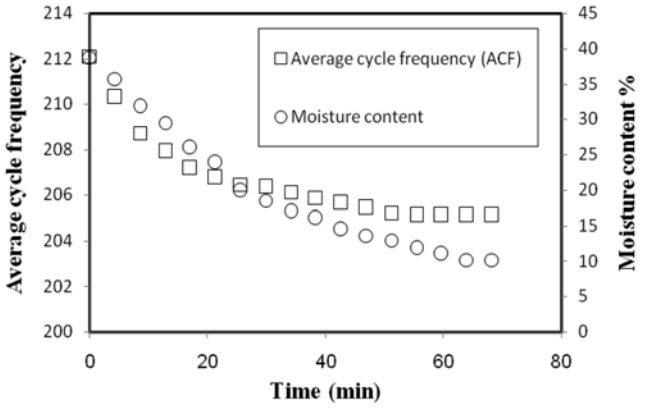

Fig. 7. Average cycle frequency values and moisture content over time.

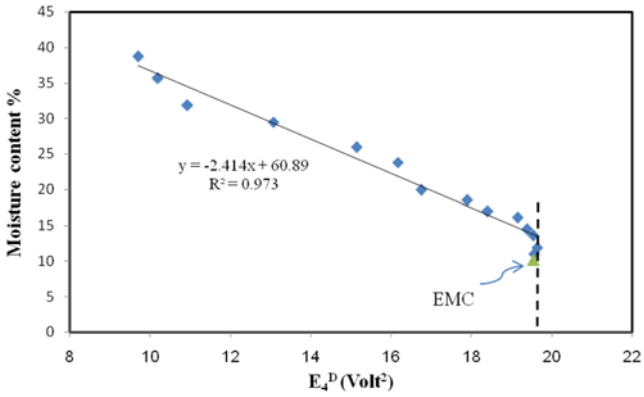

Fig. 8. Moisture content over energy of D(4).

the fluidized bed dryers in the PSDF of acoustic emissions.

During the drying process, the location of third distinct frequency shifts to lower values, while the location of other distinct frequencies does not change noticeably. A close-up of the third distinct frequency range, between 115-165 Hz, is given in the right hand side of Fig. 6. As seen, the third dominant frequency shifts approximately from 140 Hz to 130 Hz by decreasing the MC of solids.

Fig. 7 illustrates ACF and MC during the drying process. These values also decrease approximately 10 units. Decreasing of third distinct frequency and ACF confirms that the sound of the bed became more bass during the drying process.

Since the frequency in the range of 115-165 Hz, as shown in Fig. 6, is more sensitive to the change in the MC of solids than other dominant frequencies, this range was more thoroughly investigated. The corresponding raw acoustic signal was decomposed by wavelet transform into ten sub-signals. Frequency ranges of these signals are given in Table 2. As shown in there, the above-mentioned frequency range is consistent with the 4th sub-signal or D_4. Energy of this level during drying process was analyzed and illustrated in Fig. 8. This figure shows that the energy of D_4 increases by decreasing the MC. Friesen et al. [17] reported similar results. They computed the sound pressure level (proportional to the energy of sound) of raw acoustic signal and observed that the sound energy increases across the entire frequency range as the MC decreases.

This figure shows that there is a linear relationship between MC and the energy of D_4 until the EMC is reached. The linear relation is also included in this figure as well as the coefficient of determination. The coefficient of determination is near unity, indicating that there is a good correlation between this linear model and experimental data.

In addition, the energy of D_4 becomes constant by approaching the EMC. Hence, this method can be considered as a criterion for determining the MC and the end-point of the drying process. Drying operation ends while energy content of D_4 becomes constant, which is a valuable criterion for determining the overall drying time to lower MC. The same relationship can be found for other gas velocities; however, it can affect the rate of drying [26]. The same trend can be seen for other gas velocities as we discussed in the literature [27] for pressure signals.

Table 2. Frequency range of raw acoustic signal (Hz)

j	a (j)	D (j)
1	0-1024	1024-2048
2	0-512	512-1024
3	0-256	256-512
4	0-128	128-256
5	0-64	64-128
6	0-32	32-64
7	0-16	16-32
8	0-8	8-16
9	0-4	4-8

CONCLUSIONS

Passive acoustic emission signals were measured for drying of wetted rice particles in fluidized bed dryers. It was shown that the statistical analysis of the corresponding signals can be used to determine extent of constant rate zone and the falling rate zone. The peak in the frequency range of 115-165 Hz of the PSDF diagram was shown to be more sensitive to changes of the bed hydrodynamics than other peaks. Thus, wavelet analysis was used to focus on this range of frequency. Average cycle frequency of signals was used to monitor changes of the location of the peak. The frequency of this peak decreases during the drying process. Plotting the moisture content of solids against the energy of D_4 level (the same frequency range as the above-mentioned peak) helped to determine moisture content and the end point of drying. Results overall proved that analyzing the acoustic signals can be an effective nonintrusive technique to characterize the drying hydrodynamics of fluidized bed dryers.

NOMENCLATURE

a_j : approximation sub-signal
D_j : detail sub-signal
E_j^a : energy of approximation coefficient [mVolt^2]
E_j^D : energy of detail coefficient [mVolt^2]
f : frequency [Hz]
F : discrete Fourier transform [mVolt]

k : time lag coefficient
K : kurtosis
L : number of the time-series segments [-]
n : counter
N : length of the time series [-]
P^{i}_{xx} : power-spectrum estimate of each segment [mVolt^2/Hz]
P_{xx} : averaged power spectrum [mVolt^2/Hz]
s : scale factor
S : skewness
t : time [s]
w(n) : window function [-]
x_i : amplitude of the time-series signal [mVolt]

Greek Symbol

σ : standard deviation

REFERENCES

1. S. Y. Son, D. H. Lee, G. Y. Han, D. J. Kim, S. J. Sim and S. D. Kim, *Korean J. Chem. Eng.*, **22**, 315 (2005).
2. Y. H. Choung, K. C. Cho, W. J. Choi, S. G. Kim, Y. S. Han and K. J. Oh, *Korean J. Chem. Eng.*, **24,** 660 (2007).
3. W. M. Lu, S. P. Ju, K. L. Tung and Y. C. Lu, *Korean J. Chem. Eng.*, **16**, 810 (1999).
4. J. C. Schouten and C. M. Van den Bleek, *AIChE J.*, **44**, 48 (1998).
5. S. Sasic, B. Leckner and F. Johnsson, *Prog. Energy Combust.*, **33**, 453 (2007).
6. C. E. A. Finney, C. S. Daw and J. S. Halow, *Kona Powder Part. J.*, **16**, 125 (1997).
7. H. Tsujimoto, T. Yokoyama, C. C. Huang and I. Sekiguchi, *Powder Technol.*, **113**, 88 (1999).
8. J. V. Briongos, J. M. Aragón and M. C. Palancar, *Powder Technol.*, **162**, 145 (2006).
9. N. Salehi-Nik, R. Sotudeh-Gharebagh, N. Mostoufi, R. Zarghami and M. J. Mahjoob, *Int. J. Multiphase Flow*, **35**, 1011 (2009).
10. M. Abbasi, R. Sotudeh-Gharebagh, N. Mostoufi and M. J. Mahjoob, *Powder Technol.*, **196**, 278 (2009).
11. M. Abbasi, R. Sotudeh-Gharebagh, N. Mostoufi, R Zarghami and M. J. Mahjoob, *AIChE J.*, **56**, 597 (2010).
12. H. Azizpour, R. Sotudeh-Gharebagh, R. Zarghami, M. Abbasi, N. Mostoufi and M. J. Mahjoob, *Int. J. Multiphase Flow*, **37**, 788 (2011).
13. R. F. Mudde, P. R. P. Bruneau and T. H. J. J. Van der Hagen, *Ind. Eng. Chem. Res.*, **44**, 6181 (2005).
14. A. Chen, H. T. Bi and J. R. Grace, *Powder Technol.*, **177**, 113 (2007).
15. B. Demirbas, J. Nijenhuis, C. U. Yurteri and J. R. van Ommen, *Can. J. Chem. Eng.*, **86**, 493 (2008).
16. J. W. R. Boyd and J. Varley, *Chem. Eng. Sci.*, **56**, 1749 (2001).
17. T. L. Friesen, G. H. Bruswitz and R. L. Lowery, *J. Agr. Eng. Res.*, **39**, 49 (1988).
18. D. Vervloet, J. Nijenhuis and J. R. van Ommen, *Powder Technol.*, **197**, 36 (2009).
19. R. Zarghami, N. Mostoufi, R. Sotudeh-Gharebagh, J. Chaouki, L. Cheng and D. Mewes, *Nonlinear dynamic characteristic of bubbling fluidization*, Advances in Multiphase Flow and Heat Transfer. Bentham Science Publishers Ltd., **3**, 400 (2010).
20. J. Van der Schaaf, J. C. Schouten, F. Johnsson and C. M. van den Bleek, *Int. J. Multiphase Flow*, **28**, 865 (2002).
21. M. Wormsbecker, T. Pugsley and H. Tanfara, *Chem. Eng. Sci.*, **64**, 1739 (2009).
22. F. Johnsson, R. C. Zijerveld, J. C. Schouten, C. M. Van den Bleek and B. Leckner, *Int. J. Multiphase Flow*, **26**, 663 (2000).
23. S. Mallat, *IEEE T. Pattern Anal.*, **11**, 674 (1989).
24. G. Chaplin, T. Pugsley and C. Winters, *Powder Technol.*, **142**, 110 (2004).
25. A. V. Oppenheim, A. S. Willsky and S. H. Nawab, Signal and Systems, Prentice-Hall (1997).
26. K. B. Choi, S. L. Park, Y. S. Park, S. W. Sung and D. H. Lee, *Korean J. Chem. Eng.*, **19**, 1106 (2002).
27. K. Karimi, R. Sotudeh-Gharebagh, R. Zarghami and N. Mostoufi, *Dry. Technol.*, **29**, 1697 (2011).
28. R. Zarghami, *Conditional monitoring of fluidization quality in fluidized beds*, Ph.D. Dissertation, University of Tehran, Tehran, Iran (2009).